A Theory for the Spinup of Tropical Depressions

David J. Raymond, Sharon Sessions, and Željka Fuchs
Physics Department and Geophysical Research Center
New Mexico Tech
Socorro, NM 87801 USA
raymond@kestrel.nmt.edu

February 21, 2007

Summary

Recent advances in our understanding of the physics of precipitation over tropical oceans is married with vorticity dynamics to produce a simple theory for the development or non-development of tropical depressions. This early phase of tropical cyclogenesis is perhaps the least-well understood part of the whole process. The theory predicts a finite amplitude threshold for intensification, with weaker disturbances decaying. Furthermore, only disturbances with radii larger than a critical value develop. Rough estimates of this critical radius place it near 1600 km, though better estimates of various parameters could change this value significantly.

1 Introduction

The empirically determined general conditions needed for the spinup of tropical cyclones have been known for many years, i. e., warm sea surface temperatures, low environmental shear, and a pre-existing disturbance to provide low-level cyclonic vorticity (Gray, 1968; McBride and Zehr, 1981). However, in spite of the vast amount of numerical modeling work which has been done on tropical cyclones, major questions remain.

A great deal of work has gone into trying to understand the dynamical character of tropical cyclogenesis. For instance, Challa and Pfeffer (1980) and Pfeffer and Challa (1981) considered eddy angular momentum transfer from the environment into the core of a developing system. Briegel and Frank (1997) and Davis and Bosart (2003) emphasized mechanisms for the baroclinic forcing of cyclones. Simpson et al. (1997) and Ritchie and Holland (1997) discussed the role of mesoscale convective systems in cyclogenesis, while Jones (1995, 2000a,b), Frank and Ritchie (2001), and Reasor et al. (2004) investigated the effects of wind shear. Montgomery and Enagonio (1998) and Enagonio and Montgomery (2001) showed how numerous small vortices associated with individual convective events are axisymmetrized into a single larger cyclone vortex. Hendricks et al. (2004) and Reasor et al. (2005) emphasized

the role of rotating convective disturbances ("vortical hot towers") which develop in the large background vorticity characteristic of tropical cyclogenesis regions.

Somewhat less attention has been paid to the thermodynamic aspects of cyclogenesis. In a simple model Emanuel (1989, 1995) explained the finite amplitude nature of cyclogenesis seen in the simulations of Rotunno and Emanuel (1987) as a consequence of the boundary layer divergence associated with convective downdrafts in weak disturbances. Only when the middle levels became moist enough to suppress downdraft production and increase precipitation efficiency was a weak vortex able to amplify. A notable facet of the Emanuel model is the abandonment of the direct linkage of Ekman pumping to convective mass fluxes seen in many early models of cyclones, e. g., Charney and Eliassen (1964), Ooyama (1964, 1969), etc. In a model similar to Emanuel's (1989), Frisius (2006) emphasizes the importance of a negative radial gradient of precipitation efficiency in confining the convection to near the center of the cyclone vortex, a point also touched upon by Emanuel.

Gray and Craig (1998) showed exponential growth of vortex intensity from small amplitude in a simple linearized model. However, they assumed that a saturated eyewall had already formed, so their results do not necessarily contradict those of Emanuel. Zehnder (2001) also explored the effect on tropical cyclogenesis of convective forcing based on the thermodynamic principle of boundary layer quasi-equilibrium (BLQ) of moist enthalpy or entropy. He found that quite different results were obtained using this formulation in comparison to those obtained from an Ekman pumping model of convective forcing. Craig and Gray (1996) also found that a cloud-resolving model of a tropical storm did not behave in a manner consistent with the direct forcing of convection by Ekman pumping.

Using results from the TEXMEX (Tropical EXperiment in MEXico) project, Bister and Emanuel (1997) showed that hurricane Guillermo (1991) formed out of a tropical depression with a mid-level vortex overlying a moist, cold core. They found that this structure resulted from cooling by the evaporation of precipitation and hypothesized that the eventual low-level vortex apparently developed downward from the mid-level circulation.

Raymond et al. (1998) also studied the genesis of cyclones observed in TEXMEX. Using the form of the vorticity equation advocated by Haynes and McIntyre (1987), they noted that cyclone development occurs when the tendency of convergence to enhance the low-level circulation of a system defeats the tendency of surface friction to spin the system down. The "downward development" of circulation from the mid-level vortex, as envisioned by some investigators, is not supported by the Haynes-McIntyre formulation, which shows that the vertical component of vorticity undergoes only horizontal transport. The role of the mid-level vortex is more subtle in this view; it acts primarily through geostrophic (or nonlinear) balance to maintain the underlying cold core, which in turn has a thermodynamic effect on the convection occurring in this region. In particular, the cold core in conjunction with the moistening resulting from previous rainfall tends to produce a sounding profile with almost constant moist entropy (or equivalent potential temperature) above the boundary layer. An example of such a sounding taken during EPIC2001 (East Pacific Investigation of Climate, year 2001; Raymond et al. 2003, 2004) is shown in figure 1. Convection occurring in this environment is likely to have downdrafts suppressed due to the inability of subsequent rainfall to produce negative buoyancy by evaporation. The suppression of downdrafts means that the convergence at low levels associated with convective updrafts is not reduced by divergence associated with downdrafts. As a result, the low-level spinup of the system is

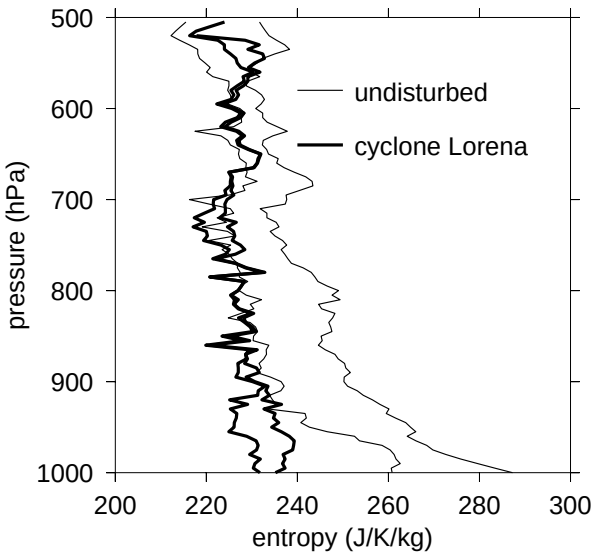

Figure 1: Dropsonde soundings taken in the tropical east Pacific on 29 September 2001. The thin lines represent undisturbed conditions at 95.01° W, 12.27° N while the thick lines show a sounding in the core of the developing tropical cyclone Lorena at 96.98° W, 9.97° N. In each case the left hand line is the specific moist entropy while the right hand line is the saturated specific moist entropy.

enhanced.

We emphasize that to cause spinup of a cyclone, low-level convergence must be associated with heating, i. e., with the latent heat release from rainfall. Without the upward export of low-level air by moist convection, convergence results in dry-adiabatic ascent and the production of a cold anomaly. The consequence is hydrostatic enhancement of the surface pressure which opposes the low pressure in the center of the vortex, resulting in spindown (see e. g. Gill 1982, p 353).

The importance of rainfall to the spinup of cyclones leads us to consider the mechanisms controlling its production. An approach based on thermodynamic principles was proposed by Raymond (2000). That paper explored the consequences of the simple postulate that mean rainfall intensity is inversely proportional to the saturation deficit, i. e., the difference between the tropospheric saturated precipitable water and the actual precipitable water. In conjunction with Neelin and Held's (1987) ideas about gross moist stability, this led to a model for the evolution of the humidity and precipitation rate in a tropospheric column.

Bretherton et al. (2004) performed a test of the hypothesis of Raymond (2000) by examining the relationship between precipitation and precipitable water over the tropical oceans, as determined by microwave measurements from SSM/I satellites. They discovered that a strong correlation exists between these quantities, but that the precise relationship varies between ocean basins. However, these differences vanished when the relationship was recast in terms of precipitation rate and saturation fraction, i. e., the ratio of precipitable water to saturated precipitable water.[1] Basically all precipitation occurs for saturation fractions between 0.6 and 0.85, with a rapidly increasing precipitation rate as a function of saturation

[1]Bretherton et al. (2004) refer to the saturation fraction as the column relative humidity.

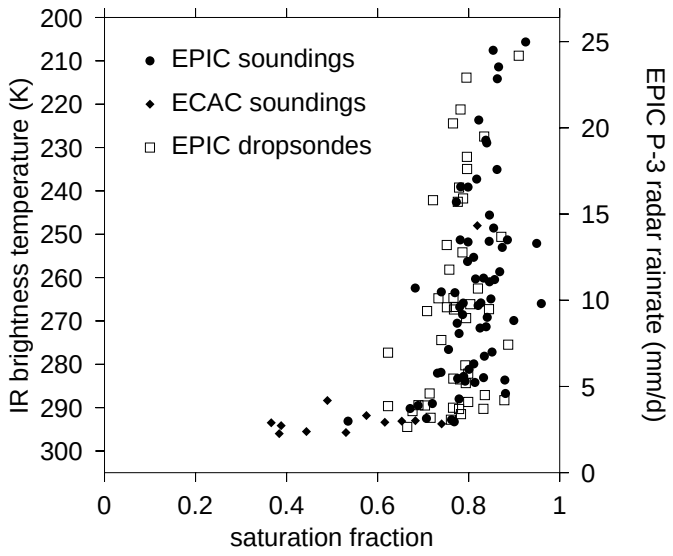

Figure 2: Saturation fraction calculated from various soundings as a function of the infrared satellite brightness temperature coincident with the sounding in time and averaged over a 50 km square centered on the sounding position. The rainfall rate inferred from airborne radar measurements corresponding to the given brightness temperatures is given on the right hand scale. This correspondence should be considered approximate, especially at high brightness temperatures.

fraction within this range. Almost no cases were found with saturation fractions exceeding 0.85.

One might expect this type of relationship to be valid for long-time averages, but to break down on shorter time scales. However, the authors found that the relation held even for daily time scales, suggesting that it reflects a fundamental physical process such as the deleterious effect of dry air entrainment on updrafts. The robust nature of this correlation is supported by figure 2, which shows saturation fraction from individual soundings in the tropical east Pacific and the SW Caribbean as a function of the coincident satellite infrared brightness temperature (considered as a proxy for precipitation) in a 50 km square centered on the sounding. In this figure EPIC soundings were launched from the ship *Ron Brown* at 95° W, 10° N in the east Pacific intertropical convergence zone, whereas EPIC dropsondes were deployed from 470 hPa by the National Center for Atmospheric Research's C-130 aircraft (Raymond et al., 2004). Only dropsondes deployed in the range 6.5° N to 12° N were used in order to limit measurements to regions of warm sea surface temperature. The ECAC soundings were launched from the Mexican research vessel *Justo Sierra* in the dry SW Caribbean during the ECAC project (Experimento Climático en las Albercas de Agua Caliente de las Américas; Magaña and Caetano, 2005).

The correlation between low infrared brightness temperature and humidity could simply be a consequence of higher humidity breeding more clouds. However, over warm ocean regions low brightness temperature generally corresponds to high stratiform cloudiness with no necessary correlation with higher humidity at low to middle levels where most of the atmospheric moisture resides. On the other hand, area-averaged precipitation rates inferred

from airborne radar data and satellite-derived infrared brightness temperature are highly correlated in the east Pacific intertropical convergence zone, with a correlation coefficient of -0.90 (Raymond et al. 2003). The scale on the right side of figure 2 indicates rainfall values corresponding to brightness temperatures in this linear regression. Thus we argue that figure 2 represents a valid, if somewhat noisy relationship between saturation fraction and precipitation rate.

More recent work by Back and Bretherton (2005) shows that some of the variance in precipitation rate at fixed saturation fraction can be explained by variations in surface wind speed, with higher wind speeds corresponding to higher precipitation rates. This result indicates that the original hypothesis of Raymond (2000) that precipitation is a unique function of saturation fraction is perhaps too simple. However, numerical simulations of convection, made in a context which we explain later, also support a strong relationship between rainfall rate and tropospheric humidity (Derbyshire et al., 2004; Raymond and Zeng, 2005). Furthermore, Derbyshire et al. show that many parametric treatments of convection in global models do not reproduce the sensitivity to moisture shown by the cumulus ensemble models.

The purpose of this paper is to marry the above ideas about precipitation and saturation fraction to the dynamics of tropical cyclones. The feedback loop which governs cyclone spinup or spindown is envisioned to be as follows:

1. The existing circulation produces surface fluxes of water vapor, moist entropy, and momentum which depend on the strength of the circulation and other environmental factors such as sea surface temperature. The moist entropy flux modifies the profile of moist entropy, and hence that of saturation fraction.

2. Convection and rainfall are considered to be governed by the saturation fraction in the convective environment inside the cyclone. Determining the dependence of convection on this environment is central to the theory of spinup.

3. The relative strengths of the spinup tendency due to low-level vorticity convergence induced by convective heating and the spindown tendency due to surface friction govern whether the cyclone vortex intensifies or decays.

We examine here only the case of weak systems such as tropical depressions in order to avoid the complications of non-linearity. In this limit we do not expect to see the warm core which is the traditional signal that a tropical storm has formed. However, this phase of intensification is arguably less-well understood than the later phases of tropical cyclogenesis.

The paper is organized as follows: Section 2 updates the theory of Raymond (2000) to account for the results of Bretherton et al. (2004), while section 3 links the updated thermodynamic results of section 2 with the vorticity dynamics of the lower troposphere as discussed by Raymond et al. (1998). In section 4 numerical results from the model of Raymond and Zeng (2005) are used to close the theory presented in section 3 and the theory is applied to an axially symmetric vortex in section 5. Conclusions are presented in section 6.

2 Thermodynamic issues

We first examine the relevant theory governing water vapor and specific moist entropy. In this theory the gross moist stability (GMS) plays a central role. The concept of GMS depends on the existence of a thermodynamic variable conserved in moist processes. Unfortunately, there is no perfectly conserved variable in this context. Neelin and Held (1987) used the moist static energy in their pioneering work on GMS, whereas Raymond (2000) used equivalent potential temperature. In this work we use the specific moist entropy, as it is easier to deal with than equivalent potential temperature. It also has somewhat better-defined conservation properties than moist static energy, though given the simplified treatment here, this advantage is not realized.

An approximate form of the specific moist entropy suitable for the present work is

$$s = s_d + Lr/T_R, \tag{1}$$

where $s_d(T, p)$ is the specific entropy of dry air, L is the latent heat of condensation (assumed constant), T_R is a constant reference temperature, and r is the water vapor mixing ratio. The specific moist entropy obeys the equation

$$\frac{\partial s}{\partial t} + \mathbf{U} \cdot \nabla s + \nabla \cdot (\mathbf{u}_i s) + \frac{\partial \omega s}{\partial p} = G + g \frac{\partial F_e}{\partial p} \tag{2}$$

where g is the acceleration of gravity, G is the irreversible generation of entropy per unit mass of air, and F_e is the vertical flux moist entropy due to diffusion, eddy transport, and radiation. We have split the horizontal velocity $\mathbf{u}$ into a solenoidal barotropic part $\mathbf{U}$ (i. e., independent of height and divergence-free) and a baroclinic part $\mathbf{u}_i$, and have taken advantage of the fact that $\nabla \cdot \mathbf{U} = 0$. We define $\mathbf{U}$ more precisely later.

We now define the pressure integral operator

$$\overline{Z} = \frac{1}{g} \int_{p_t}^{p_s} Z dp \tag{3}$$

for any $Z(p)$, where p_s and p_t are respectively surface and tropopause pressures. Applying this operator to (2) results in

$$\frac{d\overline{s}}{dt} + M\delta s = F_{es} - F_{et} + \overline{G} \tag{4}$$

where F_{es} is the surface entropy flux due to latent and sensible heat flux plus radiation and F_{et} is the upward flux of entropy out of the top of the cylinder due to radiation. The total time derivative is defined

$$\frac{d}{dt} \equiv \frac{\partial}{\partial t} + \mathbf{U} \cdot \nabla. \tag{5}$$

The second term in (4) requires further explanation. Let us define the lateral mass outflow per unit time from a column of unit area as

$$M = \frac{1}{g} \int_+ \nabla \cdot \mathbf{u}_i dp = -\frac{1}{g} \int_- \nabla \cdot \mathbf{u}_i dp, \tag{6}$$

where the plus and minus signs on the integrals indicate that only positive or negative values of the integrand are included in the integration. Due to overall mass balance, the mass flowing into the column, given by the rightmost expression in (6), equals the mass flowing out. The second term in (4) can thus be written

$$\overline{\nabla \cdot (\mathbf{u}_i s)} = \frac{1}{g}\int_{p_t}^{p_s} \nabla \cdot (\mathbf{u}_i s) dp = \frac{1}{g}\int_{p_t}^{p_s} \oint s\mathbf{u}_i \cdot \hat{\mathbf{n}}\, dl\, dp = M\delta s \tag{7}$$

where the line integral is around the periphery of the unit area defining the column, with $\hat{\mathbf{n}}$ being an outward unit normal. The quantity M is thus the mass current passing through the sides of the column in a reference frame moving with the solenoidal velocity $\mathbf{U}$, and $\delta s = s_{out} - s_{in}$ is the difference between the mean outflow and inflow values of moist entropy. The quantity δs is Neelin and Held's (1987) GMS recast in terms of the moist entropy rather than the moist static energy.[2]

An equation similar to (2) may be written for the water vapor mixing ratio r:

$$\frac{\partial r}{\partial t} + \mathbf{U}\cdot\nabla r + \nabla\cdot(\mathbf{u}_i r) + \frac{\partial \omega r}{\partial p} = -\frac{\partial}{\partial p}[(\omega+\omega_t)r_r] + g\frac{\partial F_r}{\partial p}. \tag{8}$$

The first term on the right side of this equation is the source of water vapor due to the formation and evaporation of precipitation, assuming that the horizontal and time scales are such that horizontal advection and storage of precipitation are negligible. The second term is the source due to the convergence of the vertical eddy and diffusional flux of water vapor F_r. The role of condensed water in the form of cloud droplets or small ice crystals which advect with the air is neglected in this approximate analysis.

Applying (3) to the moisture equation results in

$$\frac{d\overline{r}}{dt} - M\delta r = F_{rs} - R, \tag{9}$$

where F_{rs} is the surface evaporation rate, R is the rainfall rate, and where δr is defined as the mean inflow minus the mean outflow mixing ratio rather than the outflow minus the inflow.

We assume that $\overline{s}_d$, which is a function only of temperature, is approximately constant due to the near-invariance of the temperature profile in the tropics. It thus disappears in the time derivative in (4), leaving the first term on the left side of this equation equal to $(L/T_R)(d\overline{r}/dt)$. The mass flow M may then be eliminated between (4) and (9), leaving us with

$$(1+\gamma)\frac{d\overline{r}}{dt} = \gamma(F_{rs} - R) + \frac{T_R(F_{es} - F_{et} + \overline{G})}{L}. \tag{10}$$

Alternatively, the time derivative may be eliminated, resulting in an equation for the moisture convergence X:

$$X \equiv M\delta r = \frac{L(R - F_{rs}) + T_R(F_{es} - F_{et} + \overline{G})}{(1+\gamma)L}. \tag{11}$$

[2]Neelin and Held (1987) approximate $\overline{\nabla\cdot(\mathbf{u}_i s)}$ by $\overline{s\nabla\cdot\mathbf{u}_i}$, thus neglecting the entropy advection term $\overline{\mathbf{u}_i\cdot\nabla s}$, which is held to be negligible.

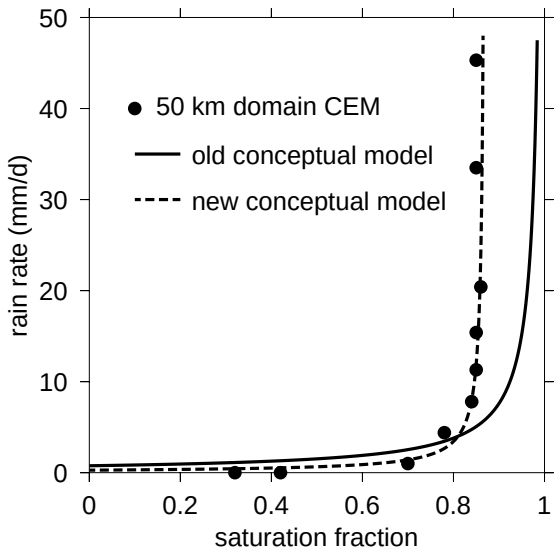

Figure 3: Relationship between rainfall rate and saturation fraction for the cumulus ensemble model on a 50 km domain, the old idealized model (solid line) and the new idealized model (dashed line).

The parameter

$$\gamma \equiv \frac{T_R \delta s}{L \delta r} = -\frac{T_R \overline{\nabla \cdot (\mathbf{u}_i s)}}{L \overline{\nabla \cdot (\mathbf{u}_i r)}} \tag{12}$$

is a dimensionless quantity closely related to the GMS. We shall refer to γ as the normalized gross moist stability (NGMS). The advantage over the GMS is that γ is a dimensionless parameter which relates the GMS (δs) to the moisture extracted (δr) and ultimately to the precipitation produced.

In a steady state, equation (10) can be solved for the net rainfall rate $R - F_{rs}$, which according to (9) also equals the moisture convergence X in this case:

$$(R - F_{rs})_{steady} = X_{steady} = \frac{T_R(F_{es} - F_{et} + \overline{G})}{\gamma L}. \tag{13}$$

This equation expresses the results of Neelin and Held (1987), and illustrates how important the NGMS is to the large-scale forcing of precipitation. For a given moist entropy imbalance, represented by the numerator on the right side of (13), the net rainfall, i. e., the rainfall minus evaporation, is inversely proportional to the NGMS in the steady state.

As it stands, (13) is a purely diagnostic relationship. To give it prognostic value, two additional pieces of information are needed; a relationship between the rainfall rate R and the precipitable water $\overline{r}$ (or saturation fraction) and a way to estimate the NGMS. We now address these issues.

So far the analysis is similar to that of Raymond (2000) except that entropy is used in place of equivalent potential temperature. The solid line in figure 3 shows graphically the humidity-precipitation relation assumed by Raymond (2000), expressed as a relationship between precipitation rate and saturation fraction. This assumption clearly does not fit

the dependence on saturation deficit of the rainfall rate predicted by the cumulus ensemble model of Raymond and Zeng (2005), which is shown by the bullets in figure 3. Nor does it agree with the form of this curve inferred by Bretherton et al. (2004) or the related data illustrated in figure 2. A much better fit is given by the dashed line

$$R = R_R \frac{S_c - S_R}{S_c - S} \tag{14}$$

where R is the rainfall rate and where the saturation fraction $S = \overline{r}/\overline{r}_s$ with r_s being the saturation mixing ratio. The quantity $S_c = 0.87$ is a critical saturation fraction corresponding to that value for which the rainfall rate goes asymptotically to infinity, while R_R and S_R are constant reference values of the rainfall rate and the saturation fraction. We find that $R_R = 4$ mm d^{-1} and $S_R = 0.81$ represent well the results of the cumulus ensemble model. This value of R_R corresponds roughly to the rainfall rate which occurs in radiative-convective equilibrium.

In the tropics the saturated precipitable water $\overline{r}_s$ is constant to the extent that the temperature profile and the surface pressure do not change. Taking the time derivative of (14) thus results in

$$\frac{dR}{dt} = \frac{R^2}{\overline{r}_s R_R (S_c - S_R)} \frac{d\overline{r}}{dt}. \tag{15}$$

Eliminating $d\overline{r}/dt$ between (10) and (15) yields a predictive equation for the rainfall rate:

$$\frac{dR}{dt} = \frac{R^2[\gamma L(F_{rs} - R) + T_R(F_{es} - F_{et} + \overline{G})]}{(1+\gamma) L \overline{r}_s R_R (S_c - S_R)} \tag{16}$$

Non-dimensionalizing, we arrive at the same equation as Raymond (2000),

$$\frac{d\alpha}{d\tau} = -\alpha^3 + \alpha^2 \Delta\phi, \tag{17}$$

where $\alpha = R/R_R$ is the rainfall rate expressed in terms of the radiative-convective equilibrium rate,

$$\Delta\phi = \frac{\gamma L F_{rs} + T_R(F_{es} - F_{et} + \overline{G})}{\gamma L R_R} \tag{18}$$

is the non-dimensional forcing, and $\tau = t/t_0$ where the scaling time t_0 is defined

$$t_0 = \frac{(1+\gamma)\overline{r}_s (S_c - S_R)}{\gamma R_R}. \tag{19}$$

The quantity $\overline{r}_s/R_R$ is just the time scale to dry out a saturated atmosphere with a steady rain equal to the radiative-convective equilibrium rainfall rate. Numbers typical of the tropics yield 15 d for this ratio. (For a similar calculation see Grabowski and Moncrieff 2004.) The factor $S_c - S_R \approx 0.06$, so the combination $\overline{r}_s(S_c - S_R)/R_R \approx 1$ d. Depending on the value of the NGMS, t_0 will be somewhat greater than this value, perhaps 3 d if, as we find later, that $\gamma \approx 0.5$.

Let us now attempt to understand what this analysis is telling us. In a steady state, the dimensionless precipitation rate equals the dimensionless forcing:

$$\alpha = \alpha_0 = \Delta\phi \qquad \text{(steady state)}. \tag{20}$$

However, in the non-steady case the rainfall rate relaxes to a steady state value as long as the NGMS $\gamma > 0$. Assuming that the rainfall rate is not too far from its equilibrium value, the time constant for this relaxation may be obtained by linearizing α in (17) about its steady-state value α_0: $\alpha = \alpha_0 + \alpha'$. The resulting linearized evolution equation is

$$\frac{d\alpha'}{d\tau} = -\alpha_0^2 \alpha', \tag{21}$$

which implies a dimensional e-folding time for relaxation of t_0/α_0^2. Thus the relaxation time becomes smaller as the steady-state rainfall rate becomes larger. For instance, if the rainfall rate is three times the radiative-convective equilibrium value then $\alpha_0 = 3$ and $t_0/\alpha_0^2 = (3/9)$ d $= 8$ h.

Moisture relaxation times of 8 h $-$ 3 d are much less than those predicted by Raymond (2000) and Grabowski and Moncrieff (2004). This is because the precipitation rate is much more sensitive to the saturation fraction at high saturation fractions than in the earlier models. These numbers compare well with the results of Sobel and Bretherton (2003) and Bretherton et al. (2004), who found relaxation times of $0.5 - 2.5$ d.

3 Vorticity dynamics

The vorticity equation in isobaric coordinates as expressed by Haynes and McIntyre (1987) and used by Raymond et al. (1998) in the study of east Pacific tropical storms is

$$\frac{\partial \zeta_a}{\partial t} + \nabla \cdot \left(\mathbf{u}\zeta_a + \hat{\mathbf{k}} \times \mathbf{F}^* \right) = 0 \tag{22}$$

where the absolute vorticity is defined

$$\zeta_a = f + \zeta = f + \frac{\partial v}{\partial x} - \frac{\partial u}{\partial y}, \tag{23}$$

f being the Coriolis parameter, and where

$$\mathbf{F}^* = \mathbf{F} - \omega \frac{\partial \mathbf{u}}{\partial p}. \tag{24}$$

The viscous and turbulent force per unit mass acting on the air is $\mathbf{F} = (F_x, F_y, 0)$. This force arises from the vertical eddy transport and diffusion of horizontal momentum and its vertical integral must be proportional to the surface stress $\mathbf{T}$:

$$\overline{\mathbf{F}} = \mathbf{T}. \tag{25}$$

We now divide the horizontal velocity into barotropic solenoidal and baroclinic parts as in section 2, $\mathbf{u} = \mathbf{U} + \mathbf{u}_i$, and use the vector identity $\nabla \cdot (\hat{\mathbf{k}} \times \mathbf{F}^*) = -\hat{\mathbf{k}} \cdot (\nabla \times \mathbf{F}^*)$ to rewrite (22) as

$$\frac{d\zeta_a}{dt} + \nabla \cdot (\mathbf{u}_i \zeta_a) - \frac{\partial F_y^*}{\partial x} + \frac{\partial F_x^*}{\partial y} = 0. \tag{26}$$

Within a weak disturbance such as a tropical depression, the absolute vorticity ζ_a is unlikely to deviate much from the environmental value in the region ζ_{ae}, which means that we can approximate the second term in the above equation by $\nabla \cdot (\mathbf{u}_i \zeta_a) \approx \zeta_{ae} \nabla \cdot \mathbf{u}_i$. In the absence of significant relative vorticity we would have $\zeta_{ae} \approx f$ where f is the Coriolis parameter, but we wish to retain the possibility that the disturbance is developing in a high vorticity region.

We wish to consider the behavior of the vorticity at low levels in an incipient cyclone, as the development of a low-level circulation is the central feature of tropical cyclogenesis. We also wish to relate the low-level convergence to the rainfall rate. One way to meet both of those goals is to make a weighted average of (26) in pressure with the weighting function being the ambient mixing ratio profile $r_0(z)$. Multiplying (26) by r_0, integrating in pressure, and dividing by $g\overline{r}_0$ results in

$$\frac{d\tilde{\zeta}_a}{dt} = \frac{\zeta_{ae} X}{\overline{r}_0} + \frac{\partial \tilde{F}_y^*}{\partial x} - \frac{\partial \tilde{F}_x^*}{\partial y} \tag{27}$$

where the moisture-weighted average

$$\tilde{Z} \equiv \int_{p_t}^{p_s} r_0 Z dp \Big/ \int_{p_t}^{p_s} r_0 dp = \frac{1}{g\overline{r}_0} \int_{p_t}^{p_s} r_0 Z dp \tag{28}$$

for any variable Z and where the moisture convergence X is approximated by $-\overline{\nabla \cdot (\mathbf{u}_i r_0)}$.

In computing the moisture convergence term we have assumed that ζ_{ae} does not vary much with height over the lower troposphere where the mixing ratio is large. For a vortex of horizontal size L this is a reasonable assumption if the vortex is in a balanced state and if the Rossby penetration depth Lf/N is greater than the scale height of the water vapor mixing ratio. (N is the typical Brunt-Väisälä frequency.) In the tropics we typically have penetration depths of order $L/300$, so systems with a horizontal scale exceeding 900 km will have penetration depths exceeding the typical 3 km scale height of water vapor.

Let us ignore the contribution of the term $-\omega(\partial \mathbf{u}/\partial p)$ to $\mathbf{F}^*$ for now (see the end of section 5) and just consider the part due to the eddy and diffusive transport of momentum. We note that

$$\tilde{\mathbf{F}} = \frac{1}{g\overline{r}_0} \int_{p_t}^{p_s} r_0 \mathbf{F} dp \equiv \frac{\hat{r}_0}{g\overline{r}_0} \int_{p_t}^{p_s} \mathbf{F} dp = \frac{\hat{r}_0 \mathbf{T}}{\overline{r}_0} \tag{29}$$

where $\hat{r}_0$ is the pressure average of r_0 weighted by the profile of the frictional force. Technically $\hat{r}_0$ is a tensor, but as long as the vertical structure of F_x and F_y are similar, then this quantity can be represented as a scalar. If surface friction is deposited in the lowest layer of the atmosphere, then $\hat{r}_0$ equals the surface mixing ratio. For deeper distributions, $\hat{r}_0$ is correspondingly less and the spindown tendency due to surface friction is weaker. Equation (27) thus simplifies to

$$\frac{d\tilde{\zeta}_a}{dt} = \frac{\zeta_{ae} X}{\overline{r}_0} + \frac{\hat{r}_0}{\overline{r}_0} \left(\frac{\partial T_y}{\partial x} - \frac{\partial T_x}{\partial y} \right). \tag{30}$$

We now identify $\mathbf{U}$ as the solenoidal part of $\tilde{\mathbf{u}}$. Since (28) weights the vertical average strongly toward low levels where the mixing ratio is largest, we think of $\mathbf{U}$ as the non-divergent part of the low-level flow. We also note that

$$\tilde{\zeta_a} = f + \frac{\partial U_y}{\partial x} - \frac{\partial U_x}{\partial y} \tag{31}$$

where $\mathbf{U} = (U_x, U_y)$. Since $\mathbf{U}$ is divergence-free, we can define a stream function ψ such that

$$U_x = -\frac{\partial \psi}{\partial y} \qquad U_y = \frac{\partial \psi}{\partial x}. \tag{32}$$

Combining this with (31) results in an inversion relation

$$\nabla^2 \psi = \tilde{\zeta_a} - f \tag{33}$$

between the low-level vorticity and stream function.

If convection is active in the lowest few kilometers of the atmosphere, then there will be a tendency to homogenize vertically the horizontal velocity in this layer. In addition, relaxation toward a balanced state will have a similar effect on the vorticity if the lateral dimensions of the incipient cyclone are sufficiently large, as discussed above. To some degree of approximation, $\mathbf{U} = \tilde{\mathbf{u}}$ then becomes not only a weighted average of the low-level wind, but approximately equal to the actual wind throughout this layer, or at least to the non-divergent part of it. Thus, we can approximate bulk surface fluxes using $U = |\mathbf{U}|$ for the near-surface wind. For surface evaporation and moist entropy flux we therefore assume

$$F_{rs} = \rho_s C \Delta r U \tag{34}$$

$$F_{es} = \rho_s C \Delta s U \tag{35}$$

where ρ_s is the surface air density, $C \approx 0.001$ is an exchange coefficient, Δr is the difference between the saturated mixing ratio at the sea surface temperature and pressure and the actual mixing ratio in the atmospheric boundary layer, and Δs is equivalent difference for moist entropy. Similarly, the surface stress is

$$\mathbf{T} = -\rho_s C U \mathbf{U}. \tag{36}$$

In the present work we assume that the surface sensible heat flux is small over the oceans, which means that the evaporation rate and moist entropy flux are approximately related by $LF_{rs} \approx T_R F_{es}$ and therefore $L\Delta r \approx T_r \Delta s$. We also assume that Δr, Δs, and C are independent of wind speed.

Equation (30) tells us that the vorticity tendency averaged over the layer of high moisture values is composed of two competing components, a part associated with moisture convergence, which tends to increase the vorticity, and a part associated with surface friction, which tends to decrease it. This by itself is no surprise. However, the analysis of the previous section provides a way for computing the moisture convergence X. In particular, (11) gives us X in terms of the rainfall rate and surface fluxes as long as the evolutionary time scale of the incipient cyclone is long compared to the moisture adjustment time scale, which we earlier estimated to be in the range 8 h – 3 d. The rainfall rate is given by (14) in terms of the precipitable water $\overline{r}$, and the evolution of the precipitable water is governed by (9) or (10). The system is thus closed if the NGMS and the surface and tropopause moist entropy fluxes are known.

4 Determination of NGMS

In this section we use the cloud-resolving cumulus ensemble model of Raymond and Zeng (2005; see also Derbyshire et al. 2004; Mapes 2004) to estimate the gross moist stability of deep convection. In this model clouds interact with their surroundings according to the ideas of Sobel and Bretherton (2000). In particular, large-scale circulations are assumed to act so as to disperse buoyancy anomalies over large areas and thus keep the mean virtual temperature profile of the computational domain close to that of the surrounding environment. This action is approximated in the model by Newtonian relaxation of the virtual temperature profile toward that of a reference profile which represents the atmosphere surrounding the convection. The strength of the cooling needed to do this is diagnosed from the relaxation, and the mean vertical velocity required to produce this cooling by dry adiabatic lifting is then inferred from the cooling rate and the dry static stability. This imagined vertical velocity and the associated horizontal flow demanded by mass continuity do not actually exist in the model since cyclic lateral boundary conditions are imposed. However, their effects are included via the imposition of moisture and moist entropy source terms consistent with this flow. Sobel et al. (2001) refer to the approximation implicit in this approach as the weak temperature gradient (WTG) approximation and we denote the above imaginary vertical velocity as the WTG vertical velocity. For shorthand we refer to the cumulus ensemble model employing this approximation as the WTG model.

In a statistically averaged sense the characteristics of the convection and the precipitation rate in the WTG model are a function of the reference profiles of temperature, humidity, and wind, the sea surface temperature, and the imposed mean surface wind. Increasing the sea surface temperature and the surface wind both increase surface heat and moisture fluxes, and hence the precipitation rate.

We have yet to explore the response of the convection to a wide variety of reference profiles. In this paper we take as a reference profile the radiative-convective equilibrium profile resulting from an imposed surface wind of 5 m s^{-1}. However, much remains to be done in exploring the full range of possible driving conditions and the results reported here are preliminary.

In the formal derivation of the WTG model governing equations, we split the horizontal and vertical velocity fields into small-scale cyclic and large-scale non-cyclic parts, $\mathbf{v} = \mathbf{v}_c + \mathbf{v}_{nc}$ and $w = w_c + w_{nc}$, with the small-scale, cyclic flow computed by the cumulus ensemble model. The large-scale part represents the above-described interaction of the model with the surrounding environment. We further assume that w_{nc} depends only on z and t. By mass continuity $\mathbf{v}_{nc}$ is therefore linear in x and y.

The convective-scale equations for specific moist entropy s and total cloud water mixing ratio r are

$$\frac{\partial \rho s}{\partial t} + \nabla \cdot (\rho s \mathbf{v}_c) + \frac{\partial \rho s w_c}{\partial z} = \rho S_e - \nabla \cdot (\rho s \mathbf{v}_{nc}) - \frac{\partial \rho s w_{nc}}{\partial z} \equiv \rho (S_e - E_e) \tag{37}$$

and

$$\frac{\partial \rho r}{\partial t} + \nabla \cdot (\rho r \mathbf{v}_c) + \frac{\partial \rho r w_c}{\partial z} = \rho S_r - \nabla \cdot (\rho r \mathbf{v}_{nc}) - \frac{\partial \rho r w_{nc}}{\partial z} \equiv \rho (S_r - E_r). \tag{38}$$

The terms involving the non-cyclic, large-scale velocities are encapsulated into E_e and E_r. These terms represent the rate at which the large-scale environment removes moist entropy

and moisture from the convective domain, and as we now show, are precisely what is needed to compute the NGMS. The terms S_e and S_r represent the local sources of entropy and moisture associated with radiation, precipitation, subgrid-scale eddy fluxes, etc.

Assuming that the density ρ is a function only of height and applying the pressure integral operator (3) to the definition of E_e, we find

$$\overline{E}_e \equiv \overline{\nabla \cdot (s\mathbf{v}_{nc})} + \overline{\frac{1}{\rho}\frac{\partial \rho s w_{nc}}{\partial z}} = \overline{\nabla \cdot (s\mathbf{v}_{nc})} - g\overline{\frac{\partial \rho s w_{nc}}{\partial p}} = \overline{\nabla \cdot (s\mathbf{v}_{nc})} \tag{39}$$

where the hydrostatic equation is invoked to change a z derivative to a p derivative. The pressure average of the pressure derivative is zero since we assume that $w_{nc} = 0$ at both the surface and tropopause. A similar relation holds for $\overline{E}_r$.

Comparing with (12) and identifying $\mathbf{v}_{nc}$ with $\mathbf{u}_i$, we note that the NGMS is simply

$$\gamma = -\frac{T_R \overline{E}_e}{L \overline{E}_r}, \tag{40}$$

where we recall that normally $\overline{E}_r < 0$. The model of Raymond and Zeng (2005) is written in terms of the equivalent potential temperature θ_e rather than the moist entropy, but using a simplified relation between the two, $s = C_p \ln(\theta_e / T_R)$, we easily find that $\overline{E}_e = C_p(\overline{E_{the}/\langle\theta_e\rangle})$ where E_{the} is the analog to E_e in the governing equation for equivalent potential temperature and where the angle brackets indicate a horizontal average over the domain of the cumulus ensemble model. Using arguments of Raymond and Zeng (2005) translated to the notation of this paper, we find that

$$E_{the} = \frac{(\langle\theta_e\rangle - \theta_{ex})}{\rho}\frac{\partial \rho w_{nc}}{\partial z} + w_{nc}\frac{\partial \langle\theta_e\rangle}{\partial z}, \tag{41}$$

where θ_{ex} equals the reference profile of equivalent potential temperature in layers of net convergence ($\partial \rho w_{nc}/\partial z > 0$) and is equal to $\langle\theta_e\rangle$ in divergent layers. The first term in (41) represents entrainment of environmental air into the convective region, while the second represents the effect of mean vertical advection. A similar expression exists for E_r.

We have computed the NGMS for a number of simulations with our WTG model. As in the case of Raymond and Zeng (2005), we make two-dimensional computations on a small, 50 km domain. Expansion of the domain to 512 km changes the results very little. The radiation scheme of Raymond (2001) is used in place of fixed radiative cooling and particle fall speeds above the freezing level are reduced from 5 m s^{-1} to 1 m s^{-1} to emulate the behavior of snow. Also, E_{the} is calculated directly via (41) rather than indirectly, with more accurate results. Other than that, the computations are identical to those of Raymond and Zeng (2005).

Figure 4 shows how the NGMS varies with wind speed and sea surface temperature (SST). Values of NGMS typically range from roughly 0.4 to 0.55 in these calculations. At fixed SST a minimum in NGMS occurs near a wind of 10 m s^{-1}. At a fixed wind speed of 7 m s^{-1} the NGMS initially decreases with an increase in SST, though this decrease is partially reversed for SST increments more than $1-2$ K above the reference value.

As a check of our calculation of NGMS, we also solve (13) for γ in the steady state

$$\gamma_{steady} = \frac{T_R(F_{es} - F_{et} + \overline{G})}{XL} = \frac{T_R(F_{es} - F_{et} + \overline{G})}{(R - F_{rs})L} \tag{42}$$

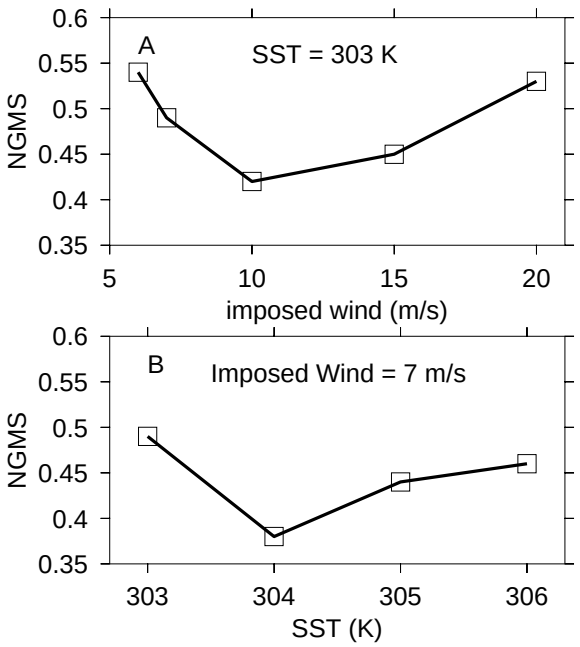

Figure 4: Plot of NGMS (a) as a function of imposed wind speed at fixed SST, and (b) as a function of SST at fixed imposed wind speed. The calculations are done using a radiative-convective equilibrium reference profile with an imposed wind of 5 m s^{-1} and an SST of 303 K.

and compare this result with that obtained using (40) and find satisfactory agreement. This equation also provides a way to determine the NGMS from observations. In situations of intense precipitation the steady-state assumption is not restrictive according to our theory, because the humidity relaxation time is typically shorter than the dynamical time scale under these conditions.

The main lesson we take away from the above results is that radiative-convective equilibrium reference profiles yield NGMS values of order 0.5. The simulations are of course very limited at this point, with a small, two-dimensional domain and no wind shear. Much needs to be done to refine and expand these calculations and to test them against observations. In particular, more general reference profiles differing from radiative-convective equilibrium need to be explored. Until more experience is gained with the WTG model, the above results must be regarded as tentative. However, as we shall see, the qualitative aspects of the theory do not depend on the precise value of the NGMS.

5 Results for an axially symmetric vortex

Insight as to how the present theory works may be obtained in a highly simplified context. We integrate (30) over a circular area A of radius a and assume axial symmetry in all quantities. We also assume provisionally that the moisture convergence is well approximated by its

steady-state value (13), resulting in

$$\frac{d\tilde{\Gamma}}{dt} = \frac{\pi a^2 \zeta_{ae} T_R \langle F_{es} - F_{et} + \overline{G} \rangle}{\gamma L \overline{r}_0} - \frac{2\pi a \hat{r}_0 |\mathbf{T}|}{\overline{r}_0} \tag{43}$$

where Γ is the relative circulation around the periphery of the area A. The angle brackets here indicate an average over the area. In addition we assume that the flow is primarily tangential to the periphery, so that the tangential component of $\mathbf{T}$ is approximately given by $|\mathbf{T}| = \rho_s C U^2$.

For the purposes of this analysis we ignore the irreversible generation of entropy and further assume that the radiative moist entropy sink is constant independent of wind speed, which is tantamount to ignoring cloud-radiation interactions. The quantity inside the angle brackets in (43) is therefore equal to the deviation of the surface flux from radiative-convective equilibrium conditions in which the imposed wind speed is U_0. Using (35), we therefore have $\langle F_{es} - F_{et} + \overline{G} \rangle \approx \rho_s C \Delta s \langle U - U_0 \rangle$.

The value of U_0 is uncertain but is likely to be approximately equal to the average surface wind speed in the tropics. As in section 4, we assume $U_0 = 5$ m s^{-1}.

We interpret U as the surface wind speed on the periphery of the area A, so that $\tilde{\Gamma} = 2\pi a U$, and assume that the mean wind speed in the interior of the area is comparable to the wind speed on the periphery U. This assumption is clearly a serious underestimate for a tropical storm, but perhaps is not so bad for a depression, which lacks a strong central vortex. Under these conditions, (43) becomes

$$\frac{dU}{dt} = \frac{U_c (U - U_0) - U^2}{D}, \tag{44}$$

where the critical velocity U_c is given by

$$U_c = \frac{a \zeta_{ae} \Delta r}{2 \gamma \hat{r}_0} \tag{45}$$

and the parameter D is

$$D = \frac{\overline{r}_0}{\rho_s C \hat{r}_0}. \tag{46}$$

Though the NGMS was shown to change somewhat with wind speed, let us assume here that it is constant. The numerical simulations in the previous section suggest a value near $\gamma = 0.5$. Then, for any intensification to be possible, we must have $U_c > 4U_0$. In this case $dU/dt = 0$ for two particular velocities,

$$U_{1,2} = [U_c \pm (U_c^2 - 4U_c U_0)^{1/2}]/2, \tag{47}$$

(where $U_1 < U_2$) and $dU/dt > 0$ only for $U_1 < U < U_2$, as illustrated in figure 5. If $U_c < 4U_0$, decay occurs for all values of U.

The condition $U_c > 4U_0$ can be recast as a condition on the system radius a:

$$a > \frac{8 \gamma \hat{r}_0 U_0}{\zeta_{ae} \Delta r} \equiv a_c. \tag{48}$$

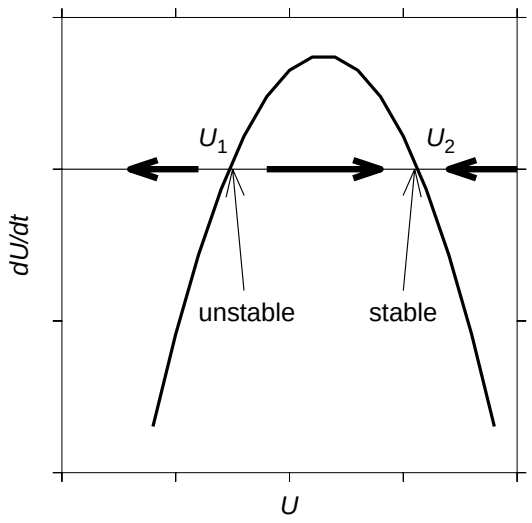

Figure 5: Schematic illustration of growth rate for an axially symmetric system. Point U_1 is a point of unstable equilibrium, while U_2 exhibits stable equilibrium. The heavy arrows indicate the direction of evolution of U with time.

The intensification of a vortex in this model thus depends on the vortex's initial size and intensity. If the radius $a < a_c$, than decay is inevitable. If $a > a_c$, then for initial peripheral tangential velocities $U < U_1$, there is decay, while intensification up to $U = U_2$ occurs for $U > U_1$. For $U > U_2$, the vortex decays to $U = U_2$.

If $\gamma = 0.5$, $U_0 = 5$ m s^{-1}, $\rho_s = 1.2$ kg m^{-3}, $\zeta_{ae} = f = 3 \times 10^{-5}$ s^{-1}, $\hat{r}_0 = 12$ g kg^{-1}, $\overline{r}_0 = 50$ kg m^{-2}, and $\Delta r = 5$ g kg^{-1}, then $a_c \approx 1600$ km and $D \approx 3500$ km. Furthermore, if as an example we take $U_c = 6U_0 = 30$ m s^{-1}, then $U_{1,2} = (3 \pm 3^{1/2})U_0$, or 6.3 m s^{-1} and 23.7 m s^{-1}. The specified value of Δr is that for 30° C sea surface temperature, 29° C air temperature, and 80% relative humidity.

The time constant for intensification can now be determined. Equation (44) can be rewritten in terms of U_1 and U_2 as

$$\frac{dU}{dt} = \frac{(U - U_1)(U_2 - U)}{D}. \tag{49}$$

The maximum growth rate occurs when $U = (U_1 + U_2)/2$, and for this value the time constant for growth is

$$\tau = \left(\frac{1}{U} \frac{dU}{dt} \right)^{-1} = \frac{2D(U_1 + U_2)}{(U_2 - U_1)^2}. \tag{50}$$

Using the above determined values, we find that $\tau \approx 8$ d. This growth time is longer than the range of possible moisture relaxation time constants, which implies that the steady state assumption for moisture convergence which is used in (43) is justified.

Let us return to the question of the neglect of the term $-\omega(\partial \mathbf{u}/\partial p)$ in the $\mathbf{F}^*$ term. By virtue of Stokes' theorem, this term contributes only on the periphery of the area A. If this area is large enough to bound the region of convection, then the periphery of A will see little or no convection, and we can assume that $\omega \approx 0$ there. On the other hand, if the periphery is embedded in the convection, then this term must be considered. Tropical

depressions tend to be cold-core at low levels, which from thermal wind considerations tells us that $\partial u_t/\partial p < 0$ where u_t is the component of the velocity in the direction of a cyclonic traverse around the area A. The contribution of this term will therefore be to retard spinup in a region of upward motion ($\omega < 0$).

6 Conclusions

In this paper a theory is developed for the early stages of the spinup of tropical cyclones. It is limited to the early development stage in order to avoid complications associated with feedback of the developing vortex on the vortex environment, i. e., non-linear effects. The theory incorporates recent advances in our understanding of the thermodynamic forcing of tropical convection and precipitation. Beyond that, it bears a strong conceptual resemblance to the simple cyclone model of Emanuel (1989, 1995) though the scales are very different.

The key assumptions of the theory are as follows: (1) cyclogenesis results when the spinup tendency of low-level convergence forced by latent heat release associated with precipitation production exceeds the spindown tendency of surface friction, and (2) precipitation is governed by the surface moist entropy flux with a small lag (several hours to a few days) and is modulated in intensity by the normalized gross moist stability.

Though numerous uncertainties exist in the details of this theory, its qualitative basis is reasonably robust. The first of the above points follows directly from the vorticity equation in flux form (Haynes and McIntyre 1987). Emanuel's (1989) model makes the second of the above assumptions and the numerical results of Craig and Gray (1996) support the hypothesis that convection is forced by surface fluxes rather than Ekman pumping.

Our focus on the role of precipitation rather than convection in cyclogenesis is appropriate because of the closer relationship of the former to low-level convergence. It is possible to have strong convection without significant low-level convergence if the convection produces strong downdrafts, as noted by Emanuel (1989, 1995). Such convection does not produce low-level spinup. However, heavy precipitation without strong low-level convergence is considerably less likely, as most of the moisture for intensely precipitating systems is drawn in laterally from the moisture-rich lower troposphere.

The lag mentioned above in key assumption two is the time required for the convective environment to moisten or dry in response to a change in the surface moist entropy flux. Ample evidence exists that the production of precipitation is exceptionally sensitive to the environmental relative humidity (Bretherton et al. 2004; Derbyshire et al. 2004; Raymond and Zeng 2005), and this considerably shortens the lag compared to simple estimates not taking this factor into account; the exact form of rainfall rate versus saturation fraction shown in figure 3 is not essential to the theory.

The idea of relating the convective mass flux and precipitation to the surface entropy flux via the gross moist stability is well established (Neelin and Held 1987; Raymond 2000), though the means for estimating the NGMS in different circumstances are relatively new and untested. Recent work not presented here suggests that moistening and stabilization of the environment act to decrease the NGMS by a factor of 2 to 3 relative to the values reported here.

More observations are needed in developing (and non-developing) cyclone precursor dis-

turbances to test the present theory. In particular, measurements of NGMS under a variety of circumstances are needed, as are observations of the vertical distribution of momentum fluxes associated with surface drag. We believe that a well-tested cumulus ensemble model run in WTG mode will eventually constitute a reliable tool for estimating the NGMS.

The theory predicts for an axially symmetric vortex that spinup can only occur if the radius of the vortex is greater than some critical value. Smaller vortices decay according to the theory. For parameter values typical of the tropical environment, the minimum radius is estimated to be 1600 km. Smaller NGMS values would decrease the critical radius. For radii greater than this value, a finite threshold for further growth exists in the tangential velocity. Vortices weaker than this threshold decay, while those stronger than the threshold intensify further.

The critical radius governs spinup because with other things being equal, the integrated precipitation rate and hence the spinup tendency over the area being considered scale with the area, whereas the frictional spindown tendency scales with the circumference, and hence the square root of the area. Thus, increasing the radius increases the spinup-spindown ratio; the critical radius is that for which this ratio equals unity.

The threshold for growth exists because the ratio of spinup and spindown tendencies $U_c(U - U_0)/U^2$ increases with surface wind speed, exceeding unity at the threshold. Recall that U_0 is the wind speed associated with radiative-convective equilibrium and U_c is a constant proportional to disturbance radius. The spinup tendency scales as $U - U_0$ since rainfall, which varies with the surface moist entropy flux and hence the wind speed, must exceed the radiative-convective equilibrium value for moisture convergence to occur.

The surface friction increases as the square of the wind speed due to the form of the bulk formula for surface stress. Because of this factor, a limit is eventually reached where the frictional spindown tendency exceeds the convergence-driven spinup tendency, and the cyclone cannot intensify beyond this limit. However, this maximum in wind speed is well into the non-linear regime where the detailed assumptions of the theory are invalid.

One factor not explored in our axisymmetric vortex model is the tendency discovered by Emanuel (1989) and examined further by Frisius (2006) for convection to expand away from the center of the cyclone in a concentric ring, thus halting cyclogenesis. This phenomenon is not addressed in our axisymmetric control volume example, but it could be accounted for in a spatially resolved version of our model by a radial gradient in the NGMS, in analogy to the precipitation efficiency gradient in the above papers.

Relaxation of some of the assumptions behind the theory allows one to explore qualitatively certain behaviors not strictly encompassed by the theory as it stands. If the atmosphere is sheared, one might expect that differentially advected dry air could make its way into the region of convection, with resulting suppression of precipitation. This would manifest itself as an increase in the NGMS and a corresponding decrease the potential for intensification. Alternatively, if the system is embedded in a region of cyclonic relative vorticity, then ingested air would have absolute vorticity larger than f, and the spinup would be enhanced. The theory is thus in essential agreement with the ideas of Challa and Pfeffer (1980) and Pfeffer and Challa (1981).

Also interesting would be to apply the theory to non-axisymmetric situations. Equations for humidity (10) and vorticity (30) along with associated diagnostic relations form a closed system assuming that the NGMS can be determined. These equations could form the

basis for studying the intensification of easterly waves and related disturbances into tropical depressions. Such an effort would be highly worthwhile, given that this may be the least-well-understood phase of tropical cyclogenesis.

Acknowledgments. We thank Daniel Martínez of the Cuban Institute of Meteorology for providing the soundings launched from the Mexican oceanographic research vessel *Justo Sierra* during the ECAC project. Two anonymous reviewers made this a much better paper via their constructive suggestions. This work was supported by U. S. National Science Foundation Grant ATM-0352639.

7 References

Back, L. E., and C. S. Bretherton, 2005: The relationship between wind speed and precipitation in the Pacific ITCZ. *J. Climate,* **18,** 4317-4328.

Bister, M., and K. A. Emanuel, 1997: The genesis of hurricane Guillermo: TEXMEX analyses and a modeling study. *Mon. Wea. Rev.*, **125**, 2662-2682.

Bretherton, C. S., M. E. Peters, and L. E. Back, 2004: Relationships between water vapor path and precipitation over the tropical oceans. *J. Climate,* **17,** 1517-1528.

Briegel, L. M., and W. M. Frank, 1997: Large-scale influences on tropical cyclogenesis in the western North Pacific. *Mon. Wea. Rev.,* **125,** 1397-1413.

Challa, M., and R. L. Pfeffer, 1980: Effects of eddy fluxes of angular momentum on model hurricane development. *J. Atmos. Sci.,* **37,** 1603-1618.

Charney, J. G. and A. Eliassen, 1964: On the growth of the hurricane depression. *J. Atmos. Sci.*, **21**, 68-75.

Craig, G. C., and S. L. Gray, 1996: CISK or WISHE as the mechanism for tropical cyclone intensification. *J. Atmos. Sci.,* **53,** 3528-3540.

Davis, C. A., and L. F. Bosart, 2003: Baroclinically induced tropical cyclogenesis. *Mon. Wea. Rev.,* **131,** 2730-2747.

Derbyshire, S. H., I. Beau, P. Bechtold, J.-Y. Grandpeix, J.-M. Piriou, J.-L. Redelsperger, and P. M. M. Soares, 2004: Sensitivity of moist convection to environmental humidity. *Quart. J. Roy. Meteor. Soc.,* **130,** 3055-3079.

Emanuel, K. A., 1989: The finite-amplitude nature of tropical cyclogenesis. *J. Atmos. Sci.,* **46,** 3431-3456.

Emanuel, K. A., 1995: The behavior of a simple hurricane model using a convective scheme based on subcloud-layer entropy equilibrium. *J. Atmos. Sci.,* **52,** 3960-3968.

Enagonio, J., and M. T. Montgomery, 2001: Tropical cyclogenesis via convectively forced vortex Rossby waves in a shallow water primitive equation model. *J. Atmos. Sci.,* **58,** 685-705.

Frank, W. M., and E. A. Ritchie, 2001: Effects of vertical wind shear on the intensity and structure of numerically simulated hurricanes. *Mon. Wea. Rev.,* **129,** 2249-2269.

Frisius, T., 2006: Surface-flux-induced tropical cyclogenesis within an axisymmetric atmospheric balanced model. *Quart. J. Roy. Meteor. Soc.*, **132**, 2603-2623.

Gill, A. E., 1982: *Atmosphere-Ocean Dynamics.* Academic Press, New York, 662 pp.

Grabowski, W. W., and M. W. Moncrieff, 2004: Moisture-convection feedback in the tropics. *Quart. J. Roy. Meteor. Soc.*, **130**, 3081-3104.

Gray, W. M., 1968: Global view of the origin of tropical disturbances and storms. *Mon. Wea. Rev.,* **96,** 669-700.

Gray, S. L., and G. C. Craig, 1998: A simple theoretical model for the intensification of tropical cyclones and polar lows. *Quart. J. Roy. Meteor. Soc.,* **124,** 919-947.

Haynes, P. H., and M. E. McIntyre, 1987: On the evolution of vorticity and potential vorticity in the presence of diabatic heating and frictional or other forces. *J. Atmos. Sci.,* **44,** 828-841.

Hendricks, E. A., M. T. Montgomery, and C. A. Davis, 2004: The role of "vortical" hot towers in the formation of tropical cyclone Diana (1984). *J. Atmos. Sci.,* **61,** 1209-1232.

Jones, S. C., 1995: The evolution of vortices in vertical shear: I: initially barotropic vortices. *Quart. J. Roy. Meteor. Soc.,* **121,** 821-851.

Jones, S. C., 2000a: The evolution of vortices in vertical shear: II: large-scale asymmetries. *Quart. J. Roy. Meteor. Soc.,* **126,** 3137-3159.

Jones, S. C., 2000b: The evolution of vortices in vertical shear: III: baroclinic vortices. *Quart. J. Roy. Meteor. Soc.,* 3161-3185.

Magaña, V., and E. Caetano, 2005: Temporal evolution of summer convective activity over the Americas warm pools. *Geophys. Res. Letters*, **32**, doi:10.1029/2004GL021033.

Mapes, B. E., 2004: Sensitivities of cumulus-ensemble rainfall in a cloud-resolving model with parameterized large-scale dynamics. *J. Atmos. Sci.,* **61,** 2308-2317.

McBride, J. L., and R. Zehr, 1981: Observational analysis of tropical cyclone formation. Part II: Comparison of nondeveloping versus developing systems. *J. Atmos. Sci.,* **38,** 1132-1151.

Montgomery, M. T., and J. Enagonio, 1998: Tropical cyclogenesis via convectively forced vortex Rossby waves in a three-dimensional quasigeostrophic model. *J. Atmos. Sci.,* **55,** 3176-3207.

Neelin, J. D., and I. M. Held, 1987: Modeling tropical convergence based on the moist static energy budget. *Mon. Wea. Rev.,* **115,** 3-12.

Ooyama, K., 1964: A dynamical model for the study of tropical cyclone development. *Geofísica Internacional*, **4**, 187-198.

Ooyama, K., 1969: Numerical simulation of the life cycle of tropical cyclones. *J. Atmos. Sci.,* **26,** 3-40.

Pfeffer, R. L., and M. Challa, 1981: A numerical study of the role of eddy fluxes of momentum in the development of Atlantic hurricanes. *J. Atmos. Sci.,* **38,** 2393-2398.

Raymond, D. J., 2000: Thermodynamic control of tropical rainfall. *Quart. J. Roy. Meteor. Soc.,* **126,** 889-898.

Raymond, D. J., 2001: A new model of the Madden-Julian oscillation. *J. Atmos. Sci.,* **58,** 2807-2819.

Raymond, D. J., C. López-Carrillo, and L. López Cavazos, 1998: Case-studies of developing east Pacific easterly waves. *Quart. J. Roy. Meteor. Soc.,* **124,** 2005-2034.

Raymond, D. J., and X. Zeng, 2005: Modelling tropical atmospheric convection in the context of the weak temperature gradient approximation. *Quart. J. Roy. Meteor. Soc.,* **131,** 1301-1320.

Raymond, D. J., G. B. Raga, C. S. Bretherton, J. Molinari, C. López-Carrillo, and Ž. Fuchs, 2003: Convective forcing in the intertropical convergence zone of the eastern Pacific. *J. Atmos. Sci.*, **60**, 2064-2082.

Raymond, D. J., S. K. Esbensen, C. Paulson, M. Gregg, C. S. Bretherton, W. A. Petersen, R. Cifelli, L. K. Shay, C. Ohlmann, and P. Zuidema, 2004: EPIC2001 and the coupled ocean-atmosphere system of the tropical east Pacific. *Bull. Am. Meteor. Soc.,* **85,** 1341-1354.

Reasor, P. D., M. T. Montgomery, and L. F. Bosart, 2005: Mesoscale observations of the genesis of hurricane Dolly (1996). *J. Atmos. Sci.,* **62,** 3151-3171.

Reasor, P. D., M. T. Montgomery, and L. D. Grasso, 2004: A new look at the problem of tropical cyclones in vertical shear flow: Vortex resiliency. *J. Atmos. Sci.,* **61,** 3-22.

Ritchie, E. A. and G. J. Holland, 1997: Scale interactions during the formation of Typhoon Irving. *Mon. Wea. Rev.,* **125,** 1377-1396.

Rotunno, R., and K. A. Emanuel, 1987: An air-sea interaction theory for tropical cyclones. Part II: Evolutionary study using a nonhydrostatic axisymmetric numerical model. *J. Atmos. Sci.,* **44,** 542-561.

Simpson, J., E. Ritchie, G. J. Holland, J. Halverson, and S. Stewart, 1997: Mesoscale interactions in tropical cyclone genesis. *Mon. Wea. Rev.,* **125,** 2643-2661.

Sobel, A. H., and C. S. Bretherton, 2000: Modeling tropical precipitation in a single column. *J. Climate,* **13,** 4378-4392.

Sobel, A. H., J. Nilsson, and L. M. Polvani, 2001: The weak temperature gradient approximation and balanced tropical moisture waves. *J. Atmos. Sci.*, **58**, 3650-3665.

Sobel, A. H., and C. S. Bretherton, 2003: Large-scale waves interacting with deep convection. *Tellus,* **55a**, 45-60.

Zehnder, J. A., 2001: A comparison of convergence- and surface-flux-based convective parameterizations with applications to tropical cyclogenesis. *J. Atmos. Sci.,* **58,** 283-301.